Additive Process Using Femto-second Laser for Manufacturing Three-dimensional Nano/ Micro-structures

Dong-Yol Yang[1,#], Tae Woo Lim[1], Yong Son[1], Hong-Jin Kong[2], Kwang-Sup Lee[3], Dong-Pyo Kim[4] and Sang Hu Park[5]

1 Dept. of Mech. Eng., KAIST, Guseong-Dong, Yuseong-Gu, Daejeon, South Korea, 305-701
2 Dept. of Phys., KAIST, Guseong-Dong, Yuseong-Gu, Daejeon, South Korea, 305-701
3 Dept. of Polymer Sci. and Eng., Hannam University, Ojeong-Dong, Daedeok-Gu, Daejeon, South Korea, 306-791
4 Dept. of Fine Chemical Eng. and Chem., Chungnam National University, Gung-Dong, Yuseong-Gu, Daejeon, South Korea, 305-764
5 School of Mech. Eng., Pusan National University, Jangjeon 2(i)-Dong, Geumjeong-Gu, Pusan, South Korea, 609-735
Corresponding Author / E-mail: dyyang@kaist.ac.kr, TEL: +82-42-869-3214, FAX: +82-42-869-5214

KEYWORDS : Two-photon stereolithography, Three-dimensional nano/micro structures

The two-photon stereolithography (TPS) process is a promising technique for the fabrication of real three-dimensional (3D) nano/micro-structures via application of a femto-second laser. In TPS, when a near-infrared ultrashort-pulsed laser is closely focused onto a confined volume of photocurable resin, only the local area at the center of the focus is cured. Therefore, real 3D microstructures with resolution under the diffraction limit can be fabricated through a layer-by-layer accumulative technique. This process provides opportunities to develop neo-conceptive nano/micro devices in IT/BT industries. However, a number of issues, including development of effective fabrication methods, highly sensitive and functional materials, and neo-conceptive devices using TPS, must be addressed for the realization of industrial application of TPS. In this review article, we discuss our efforts related to TPS: effective fabrication methods, diverse two-photon curable materials for high functional devices, and applications.

Manuscript received: September 10, 2007 / Accepted: September 13, 2007

1. Introduction

Recently, precise fabrication technologies such as photolithography, imprinting, deposition, and etching have taken on greater importance in many areas of modern industries, including applications of integrated circuits, information storage devices, photonic devices, miniaturized sensors, microfluidic devices, biochips, and semiconductors.[1-3] In efforts to obtain higher efficiency and realize neo-conceptive devices, a number of research works involving fundamental technologies such as actuating, positioning, and sensing have been carried out for the fabrication of two/three-dimensional (2D/3D) nano/micro structures.[4-8] In addition, some nano/micro processes that overcome the limits of the conventional processes have been proposed.[9-17] X-ray and extreme ultraviolet were employed to improve the resolution of photolithography. Direct writing using a sharp pen, an electron beam, and a focused ion beam (FIB) provide ultra precise patterns with several or several tens nanometers scale. Self-assembly and holographic lithography are advantageous for the mass production of 2D and 3D regular structures of particles, while masked etching and deposition methods followed by the aforementioned pattering processes make it possible to pattern diverse materials. However, most of the processes thus far developed do not enable the fabrication of arbitrary 3D microstructures.

The two-photon stereolithography (TPS) process is recognized as a useful method for the fabrication of real 3D micro structures.[18-21] In the past decade, a number of studies on TPS induced with a femtosecond laser have been carried out. It is known that a femto-second laser pulse can be closely focused onto two-photon curable resins. The probability of two-photon absorption occurs nonlinearly, in proportion to the square of the photon intensity. Therefore, the local area around the center of the focused laser beam cures as a result of absorption of the threshold energy. The resolution of a unit volume pixel (voxel) is smaller than the diffraction limit of the laser beam, close to 100 nm in size.[22] The development of prototypes of 3D micro devices such as micro oscillators, photonic crystals, and micro needles demonstrates the potential of TPS.[23,24]

However, problems related to improvement of precision, mass production, and diversity of materials must be resolved in order to allow for the realization of industrial applications of TPS.[25-30] In this review paper, recent research activities related to TPS performed by our group are discussed. The principles and processes are introduced in section 2. In section 3, effective fabrication methods are discussed. Section 4 shows 3D fabrication using diverse materials. Molding and pattern transplanting techniques for mass-production are proposed in Section 5. In section 6, one promising application, 3D micro-channels, is introduced.

2. Two-photon Stereolithography

2.1 Mechanism of two-photon curing

Two-photon absorption (TPA) is a nonlinear optical phenomenon wherein an electron transits from a low energy level to an upper energy level by absorbing two photons simultaneously. The energy of a photon is given by $\hbar\omega$, where $\hbar$ and ω are Flank's constant divided by 2π and the light angular frequency, respectively. The electron can be transited once it absorbs the energy of a single photon, which is equal to $\hbar\omega = E_1-E_2$, where E_1 and E_2 are the energy levels. In the case of TPA, two photons with energy of $(E_1-E_2)/2$ per photon cause the electron to transit. However, the cross-section of TPA is much smaller than that of the single photon absorption, and thus TPA is induced only when high power light is illuminated. A Ti:Sapphire laser is widely used for TPA, because it produces an ultra-high power pulse with a pulse width of several tens of femtoseconds or less. Furthermore, it is very useful for TPS, because it has a center wavelength of around 800 nm, half of which is close to the critical wavelength for the polymerization. This lends easy control of the threshold energy for curing, as well as over the size of the unit volume.

2.2 Two-photon stereolithography system

Recently, actuating and sensing elements have been studied intensively, and diverse scanning systems of nano-precision have been developed.[32-35] TPS systems can be grouped into two categories according to the scanner type employed. Figures 1(a), (b) show schematic diagrams of TPS systems: a Galvano scanning type and a piezoelectric stage type, respectively. Both systems provide several nm resolution. Although the Galvano scanning type provides high response time and is simple to control, the stage scanning type is advantageous for fabrication over a large area of several hundred micrometers.

A mode-locked Ti:sapphire laser, which has an 780nm wavelength, 80MHz repetition, and less than 100fs pulse width, is employed as a source. The beam is then focused vertically with an objective lens (NA, numerical aperture 1.5; x 100) using the piezoelectric stage along the z-axis. The exposure time of the beam is controlled by a galvano-shutter with a stable response time of 1ms. The resolutions of the scanner and the z-stage are 24nm and 100nm, respectively. The shutter, the scanner, and the PZT z-stage were controlled by a computer system. The situations of fabrication progress can be monitored exactly using the high magnifying CCD camera.

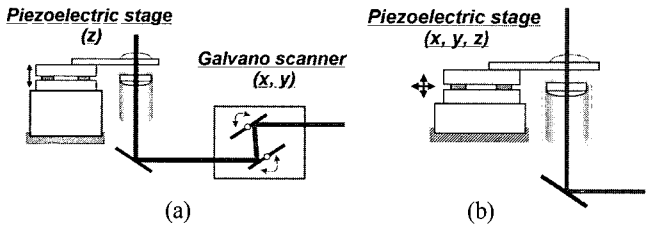

Fig. 1 Schematic diagrams of (a) the beam-scanning and (b) the stage-scanning systems

3. Improvement of Fabrication Efficiency

3.1 Nano-surfacing process

3D nanofabrication using TPS utilizes the general method of layer-by-layer accumulation of 2D scanning paths of the laser beam, where the paths are obtained from sliced 3D CAD data. Accordingly, the process requires much time to build up complex 3D microstructures. We proposed a novel method, named nano-surfacing process (NSP), to fabricate 3D concavo-convex microstructures employing TPS with a single-layer method for high fabricating efficiency.[25] In the NSP, a 2D bitmap figure is divided into several subregions having the same height horizontally. The figure is then transformed into a multi-voxel matrix (MVM); in the MVM, contours with identical height express a character number. It is well known that the height and diameter of a voxel are controlled by the laser dose, and thus it is possible to express 3D concavo-convex shapes using the different heights of voxels. Therefore, in the MVM scanning method, different laser doses are exposed onto the resin according to character numbers of the MVM in order to fabricate 3D concavo-convex shapes.

Eq. 1, which expresses the voxel length as a function of the system conditions and process parameters at the focus of the laser beam, is employed to obtain the equation of the process parameters for a given height.

$$l(P,t) = 2z_{r=0} = \frac{2\pi w_0^2}{\lambda} \times \left\{ \left(\frac{4P^2 t}{\pi^2 w_0^4 E_{th}} \right)^{\frac{1}{2}} - 1 \right\}^{\frac{1}{2}} \quad (1)$$

where λ, E_{th}, w_0, P, and t are the wavelength, the threshold energy for photopolymerization, the beam radius at the focus, the laser power, and the exposure time, respectively. λ, E_{th}, and w_0, are determined by the system conditions. E_{th} is an experimental constant influenced by the properties of the resin and the laser beam, and w_0 is a constant influenced by the characteristics of the objective lens and the laser beam.

From (1), the relationship between exposure time and voxel length is a fourth-order polynomial expression. Therefore, the exposure time can be represented as an approximate expression using the experimental results, the variation of voxel length according to the process parameters, as expressed in (2) as follows:

$$t(l) = Al^4 + Bl^3 + Cl^2 + Dl^4 + E \quad (2)$$

where A, B, C, D, and E denote constants depending on the system conditions; they can be obtained on the bases of the experimental results.

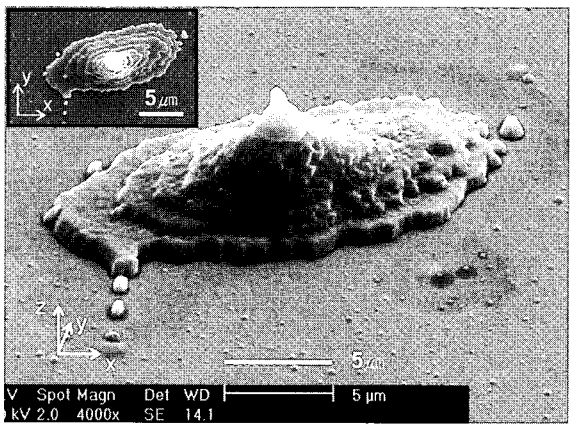

Fig. 2 SEM image of fabricated island with exaggerated ratio of height vs. width by controlling both exposure time and laser power simultaneously. Inset is top view of the structure[25]

As a complex example, we have attempted to fabricate Jeju Island, the largest island in Korea. The island shape is convex in perspective, and hence it can be fabricated using the NSP. A bitmap figure of Jeju Island expressed as 10 sub-regions is obtained from a real topographical map of the island. Figure 2 shows the island fabricated with an exaggerated ratio of height vs width. A structure with 5 ㎛ height difference and the same width is fabricated by controlling the process parameters between 80 mW, 1 ms and 280 mW, 2 ms. The results show that the MVM scanning method is an effective means of fabricating a 3D surface with various aspect ratios. The result shows that it readily enables the fabrication of single-layered 3D microstructures.

3.2 Multi-path scanning method

To date, the deformation due to the surface tension between a rinsing material and solidified microstructures during the developing process has been a major problem in TPS. Generally, the surface tension significantly affects the precision of the resulting 3D microstructures. A simple and effective laser scanning method to reinforce the strength of 3D microstructures without loss of precision was proposed to address this problem. [21, 36, 37]

The cause of pattern collapse is generally known to be a centrifugal force induced by the surface tension of a developing material during the drying process. There are two basic laser scanning methods to fabricate 3D microstructures via TPS: the raster scanning method (RSM) and contour scanning method (CSM). CSM uses only outer-contour scanning for polymerization, leaving the inside contours in an unpolymerized state; in contrast, in the case of RSM, all voxels in a volume that contains 3D microstructures are scanned and polymerized. For this reason, CSM requires a relatively small number of voxels for 3D fabrication. It is therefore a more effective means of fabricating 3D microstructures and is popularly used in 3D microfabrication based on TPS. However, with CSM, the shell thickness of the solidified contours is generally very thin, approximately 150 to 200 nm, due to a minimized voxel size that permits precise fabrication. Hence, microstructures fabricated by CSM are easily deformed during the developing process. The mechanical strength of a structure is generally increased in proportion to the cube of its thickness, and thus the thickness of a 3D microstructure is an important factor for successful fabrication via CSM. Essentially, the height of a voxel is enlarged depending on the increase of the laser dose from h to H, and an extra-shape appears due to expansion of the voxel diameter. These factors becomes obstacles to precise fabrication in the layer-by-layer accumulation approach.

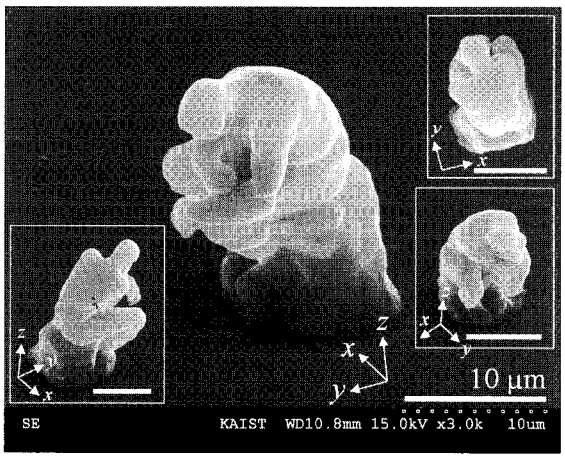

Fig. 3 SEM images of fabricated micro-Thinker by double-scanning path. The insets are the same micro-Thinker with various view angles, and the scale bars are 10 μm [21]

The multi-path scanning (MPS) method is an alternative approach that provides effective reinforcement of strength of 3D microstructures without a reduction of the resolution. The multi-path is obtained strictly from 2D sliced data by using a Voronoi diagram. Through reiteration of this procedure, three or more scanning paths can be generated precisely in the interior of the sliced data with the same distance as the offset. The important advantages of MPS are that the contours can become continuously thicker toward their inner side without a reduction of precision, and that the target thickness of a contour can be obtained simply by controlling the offset distance between contours and the number of inner contours. The optimal offset between contours can be evaluated experimentally.

'Micro-Thinker', scaled down to 1:93,000 as compared with the original sculpture by Rodin, was fabricated via the MPS method with an offset of 150 nm; this was the optimal value under a laser power of 40 mW and exposure time of 1 ms per voxel, as shown in Fig. 3. The MPS method provides precise fabrication of diverse 3D microstructures without any distortions.

4. Ceramic Micro-fabrication

4.1 Ceramic micro-fabrication using a ceramic precursor

In spite of advantages related to their chemical and mechanical properties, ceramic materials are not normally utilized for the fabrication of nano/micro devices due to difficulties in processing these materials. Recently, a precursor process based on a sequential curing and heating process was proposed for 3D ceramic microfabrication. 3D microstructures were fabricated by utilizing different established nano/micro fabrication processes with UV or thermal curable polymeric precursors, and the polymeric microstructures were then transformed into ceramic microstructures through a heating process.[38-40]

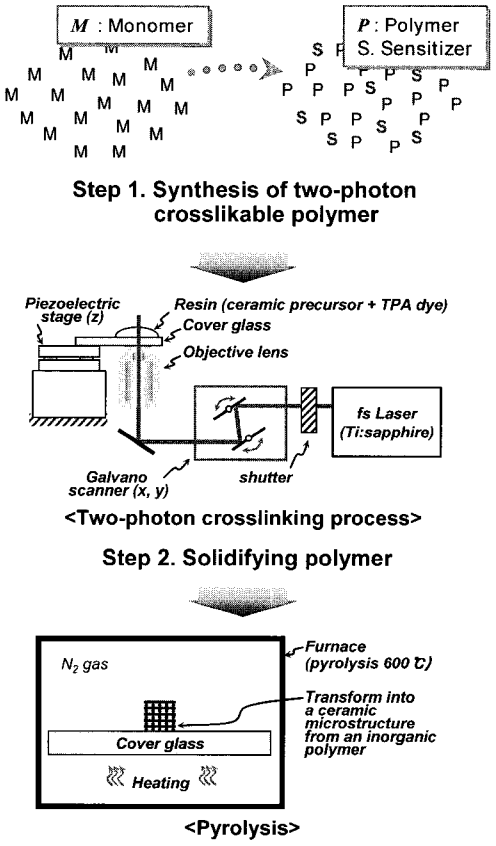

Fig. 4 The whole process for the 3D ceramic microstructures using ceramic precursors

Regarding precursor processes, the direct fabrication of 3D ceramic structures with a high spatial resolution has been demonstrated using a polymeric ceramic-precursor that is crosslinked by two-photon absorption for 3D shaping and is transformed to the SiCN ceramic state by pyrolysis. This process paves the way for the direct fabrication of complex 3D ceramic microstructures with a resolution of near 200 nm. It also has considerable potential for the fabrication of various innovative ceramics that would otherwise be fabricated via mechanical machining, molding, or photolithography. Figure 4 illustrates the whole process for obtaining 3D ceramic microstructures using ceramic precursors.

4.2 Ceramic microstructures

An inorganic polymer photoresist was synthesized via functionalization of polyvinylsilazane (VL-20, KiON) with 2-Isocyanatoethyl methacrylate, which has many vinyl groups and methacrylate units, as a precursor of SiCN ceramic.[26] The photosensitivity of the synthesized resin was comparatively evaluated

by measuring the UV-absorbance spectrum and photo-DSC thermogram, and substantially improved photosensitivity was confirmed.

The elastic modulus with variation of pyrolysis temperature was observed. The modulus of the UV-cured polymer films was kept around 4 GPa with nearly no change upon heating to 500℃; there was a steep increase of the Young's modulus to ~30 GPa for a sample annealed at 600℃. This clearly indicated that the polymer pyrolyzed at a temperature over 600℃ became a ceramic material in terms of mechanical behavior. Moreover, the film strength was further increased up to 60 GPa at 800℃, which is similar to the strength of reported polymer-derived ceramics. However, pyrolysis was conducted until 600℃ considering the deformation of the substrate, i.e., coverglass.

A developed inorganic polymer photoresist containing 0.4 wt% photosensitizer of TP-Flu-TP2 was selectively consolidated via a two-photon absorbed photocross-linking route, while the initial polyvinylsilazane was not two-photon curable. The smallest line width of 210 nm was achieved under a laser power of 100 mW and duration time of 1 ms; this resolution is comparable to cases where other two-photon materials were used.

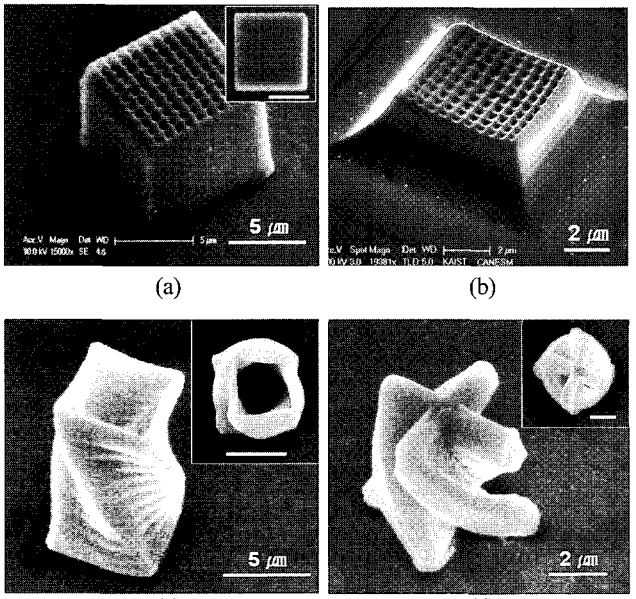

(a) (b)

(c) (d)

Fig. 5 (a) Polymeric woodpile structure with no filler, (b) ceramic woodpile structure with no filler after pyrolysis. Alternative 3D ceramic microstructures of spiral (c) microtube and (d) microshaft, fabricated using the 40 wt% particle containing resin[26]

The fabrication of a real 3D ceramic woodpile structure with 9㎛ x 9㎛ x 9㎛ dimensions was performed by accumulating line patterns layer-by-layer. However, after pyrolysis at 600℃, the photocured woodpile structure was significantly deformed into a pyramid-like structure that was nonlinearly tapered along the perpendicular direction, as shown in Figs. 5(a) and (b). To address the shrinkage problem, silica particles with approximately 10 nm diameter were introduced as a filler into the inorganic polymer photoresist resin with various solid loading portions. Here, it was verified that the shrinkage could generally be reduced with a linear relation of $41(1-\delta)\%$ for the silica particle portion (δ). In addition, the ceramic structure containing 40wt% silica particles exhibited isotropic shrinkage owing to free sliding from the substrate during pyrolysis, presumably due to weak interfacial adhesion to the substrate. The spiral microtube and cruciform shown in Figs. 5(c) and (d) were also fabricated using the developed resin polymer mixed with 40 wt% silica particles, suggesting novel applicability of these structures for chemical channels or for use in mechanical devices. These preliminary results indicate that the proposed approach, in combination with newly developed photoresist resins as different ceramic precursors, as well as a wide selection of fillers and fabrication processes, can lead to the realization of unique 3D ceramic structures with enhanced structural complexity and excellent dimensional stability for a variety of applications in the fields of tribological MEMS and chemical resistant microfluidics.

5. 3D Molding and Pattern Transferring Techniques

5.1 3D nano-imprinting

Long processing time is normally required to create 3D microstructures due to the intrinsic TPS characteristic of layer-by-layer accumulation. For this reason, TPS, although capable of affording unique 3D micro- and nanoscale structures, is considered to be incompatible with mass production. Therefore, increasing the throughput of TPS has recently moved to the forefront of research in efforts to promote the practical use of TPS as a nanofabrication process.[27] The single-step fabrication of 3D or multilevel structures offers a multitude of benefits. Inherent in this approach is the elimination of need for alignment in multilevel fabrication. Furthermore, it is a cost effective, simple process. For 3D UV-NIL, a trial in the fabrication of multilayered stamps has been conducted, employing two-photon polymerization and a diamond-like carbon (DLC) coating technique.

An approach using an O_2-plasma cleaner (this was originally utilized for surface treatment and cleaning) as a secondary process for improving the resolution of microstructures created by TPS has been proposed. The polymerized patterns created by TPS can be sharpened in an atmosphere of O_2 plasma. The ashing rate η is about 36.6 nm/min defined as $\eta = (\omega_0 - \omega_f)/t$, where wo and wf indicate the original and thinned linewidths after the plasma ashing, respectively

After the ashing process, the stamp for UV-NIL is coated by a DLC coating technique in order to obtain lower friction, lower surface energy, and higher hardness. The thickness is optimized considering the hardness and UV transparency. Figure 6 shows fabricated 3D concavo-convex multilayered stamps as well as their corresponding UV imprinted results. From the results, excellent correlations between 3D mutilayered stamps and imprinted features can be observed. This indicates that multilevel nano- and microscaled structures can be created in a single step using multilayered stamps.

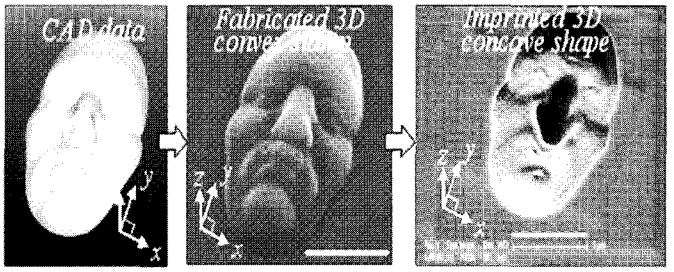

Fig. 6 Schematic sequential procedures of creating 3D face shape from designed shape to imprinted result: computer-aided design (CAD), SEM image of fabricated 3D convex face shape stamp, the scale bar is 5 ㎛, and 3D concave shape of imprinted result[27]

5.2 Fabrication of 3D ceramic Mold

A method for the fabrication of 3D SiCN-based ceramic molds for the stamp of hot-embossing process was studied.[28] The ceramic stamp is fabricated by a sequential process involving the fabrication of polymer master patterns and PDMS molds, micro-molding using a preceramic polymer, and a pyrolysis process. After polymerization by TPS, the liquid resin is removed by ethanol in a developing process. Following this, a concave PDMS mold is obtained by a casting process. The ceramic precursor is then spread onto the patterned surface of the PDMS molds fabricated from two master patterns. Viscous polyvinylsilazane (Kion® VL20) is used as a precursor of the SiCN ceramic. The excess polymer is scraped away using a piece of flat PDMS, leaving a filled PDMS mold. The filled mold is then

brought into contact with a Si wafer, and the polymeric precursor is cured under a UV-light for 20 min with an intensity of 10 mW/cm^2 at room temperature. The PDMS mold is then removed by either peeling it from the substrate or dissolving it with a 1.0 M tetrabutyl-ammonium fluoride (TBAF) solution in tetrahydrofuran (THF) at room temperature. Both methods were performed without yielding defects in the polymeric structures. All of the processes are carried out in an inert gas atmosphere to avoid exposure to moisture. The patterned polymeric microstructures are transferred into a tube furnace and heated to 800℃ at a rate 2℃/min. Through the entire process, 3D SiCN ceramic micropatterns were obtained due to the phase transition during pyrolysis.[28]

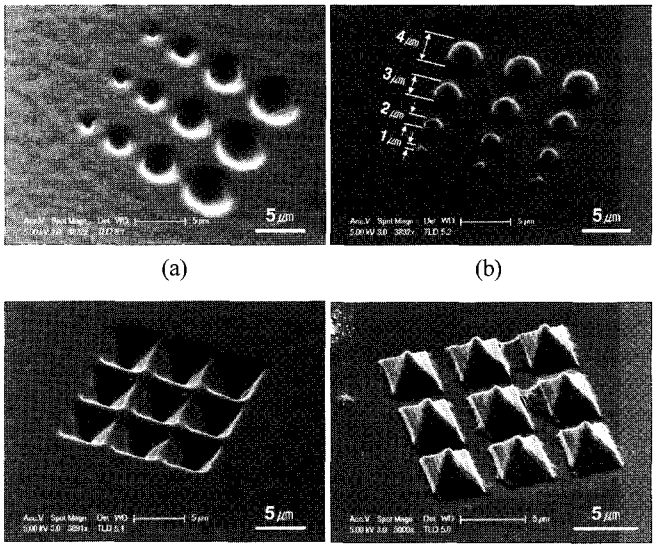

Fig. 7 SEM images of fabricated PDMS molds, and SiCN ceramic structures fabricated by soft molding. (a), (c) The figures on the left side are PDMS molds, while (b) and (d) on the right side are replicated SiCN ceramic structures

Figures 7(a) and (c) show PDMS molds whose master patterns were fabricated using the nSL process, and Figs. 7(b) and (d) show SiCN ceramic structures created by micro transfer molding using PDMS molds. In this case, various patterns can be fabricated within submicron resolution; this constitutes a considerable improvement compared to earlier research in the area of fabrication of ceramic microstructures. Figs. 7(b) and 7(d) show multi-scale hemisphere patterns with a diameter of 1~4 μm, as well as pyramid patterns. The curved sides of the pyramid patterns, owing to shrinkage during pyrolysis, illustrate that the shrinkage can help improve the sharpness of a probe. The 3D SiCN-based ceramic micropatterns can be applied to various areas, such as the mold of a hot embossing process or mechanical and chemical devices used in harsh environments.

5.3 Adaptive bonding technique

Placing 3D microstructures on opaque substrates, such as silicon wafers and metal layers, regardless of surface flatness, and on microsystems provide diverse applications with realization of specific functions in the system. Although direct fabrication of 3D microstructures on opaque materials and inside systems containing macroscale components should be possible using TPS, precisely controlling a tightly focused beam on a large area with a nanostage is generally cost prohibitive. Furthermore, most approaches require immersion oil of 1.51 refract index be placed in front of the objective lens so as to increase the numerical aperture and generate the smallest possible spot size. A thin transparent glass plate is then necessary to isolate the immersion oil from the photocurable resin, thus explaining why most 3D microstructures have been built on thin glass plates rather than on opaque materials. As such, another approach for manipulating 3D microstructures is required. We therefore propose a contact print lithography (CPL) technique to transplant 3D microstructures fabricated by TPS onto other materials, regardless of their transparency.[29]

There are three fundamental steps when using CPL to transplant 3D microstructures onto a macroscale substrate. First, a 3D stamp is prepared for contact printing. A self-assembled monolayer (SAM) is then vapor-deposited onto the glass plate using an ion method to reduce the adhesive force between it and the 3D microstructure. The reverse shape of the 3D structure is fabricated using TPS on a plate that is utilized as a carrier plate. The plate is then positioned on a substrate coated with a thin, UV curable adhesive layer, as shown in Fig. 8. To affect contact between the 3D structure and the adhesive layer, the circumference is pulled down with a 1 bar vacuum. The bonding layer is subsequently exposed to UV light to be cured and to bond the 3D structure onto the substrate, and the plate is then carefully removed.

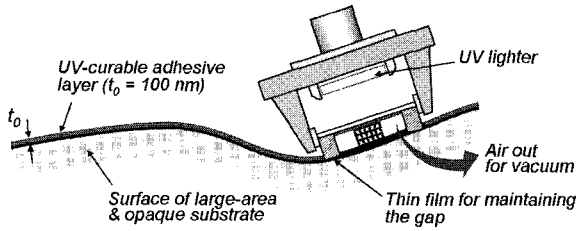

Fig. 8 When the height of a 3D microstructure was larger than the gap (film thickness), the structure buckled during CPL[29]

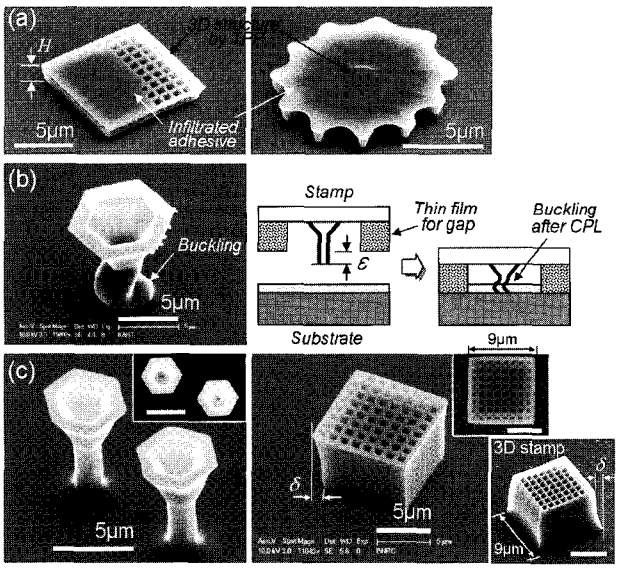

Fig. 9 SEM images of transplanted 3D microstructures on a substrate. (a) If the height (H) of the 3D structure was too small, the adhesive resin infiltrated the 3D structure by capillary forces. (b) When the height of a 3D microstructure was larger than the gap (film thickness), the structure buckled during CPL. (c) Well-standing pillars with hexagon heads and a woodpile structure by controlling the gap. The shrinkage volume (δ) shown at the top of the stamp was reverse transplanted onto the substrate. Their dimensions were not changed after CPL. The right-upper images are top views of the structures, and all scale bars are 5 μm[29]

To evaluate the usefulness of CPL, we transferred 3D microstructures onto the surface of a Si wafer. The adhesive layer on the substrate was a commercial UV-curable resin, AMO NILMMS10 (from AMO GmbH). It was spin coated to a thickness of approximately 100 nm onto the surface of the Si wafer prior to the CPL. In order to obtain good conformal contact with the 3D microstructures, the adhesive layer must be of uniform thickness, but the actual thickness is not critical within a range of 1~200 nm. If the height of the 3D structure is very low, capillary force can easily drive

the adhesive into the 3D structure during CPL, as shown in Fig. 9(a). The maximum infiltrated height (h_{max}) is dependent on a narrow gap (L) in the structure, the surface tension (γ) at the adhesive/air interface, and the contact angle (θ) at the adhesive/microstructure interface, which gives $h_{max}=2\gamma\cos\theta/\rho GL$; here, ρ is the density of the adhesive and G is the gravitational constant. Therefore, the height of 3D microstructures should be higher than the value of h_{max} for the prevention of full infiltration into the structure, with the height of 2 ㎛ of a woodpile having the gap of 700 nm, that was infiltrated to its top surface, as shown in Fig. 9(b). For the reduction of h_{max}, the adhesive must have low surface tension and high density. As shown in Fig. 9(c), the edge size of the top surface in the transplanted woodpile is also 9 ㎛. The height of the structure after CPL is reduced by as much as the amount of immersion into the adhesive layer (in this case, about 100 nm). This indicates that there is no elastic recovery of the structure after transplantation. Thus, it is evident that precise transplantation of 3D microstructures into a system is possible.

It is concluded that, using CPL, it is feasible to fabricate innovative microsystems containing 3D microstructures, such as 3D mixers or filters inside microchannels or 3D photonic crystals inside optical devices.

6. Application for 3D Micro-channels

A nano/micro hybrid process for the fabrication of 3D intelligent nano/micro-channels has been proposed. Micro-channel patterns of several millimeters were fabricated using a photolithography method, and 3D functional microstructures inside the micro-channels were fabricated by TPS utilizing a stage scanning system for large-area fabrication.

Micro-channels were patterned on a cover glass using a photo-lithography process. The thickness was controlled at 50 ㎛ by spincoating for post-processing of TPS. A two-photon crosslinkable resin was then dropped inside the channel patterns, and 3D functional microstructures for mixing were fabricated in the channel pattern via the TPS process. Finally, the pattern on the coverglass was enclosed by a slide glass with inlet and outlet holes for fluids. For good adhesion between the plates, a photo resist was spin-coated on the slide glass before covering. SU-8, one of the most robust two-photon crosslinkable resins, was employed for the fabrication of 3D microstructures in a large scale. This is important because critical 3D pattern deformations may arise as a result of surface tension on the developer during the developing process. SU-8 was employed in the other process in order to improve adhesion between the 3D structures and the channels. In addition, SU-8 has good chemical, mechanical, and bio-compatible properties.[23]

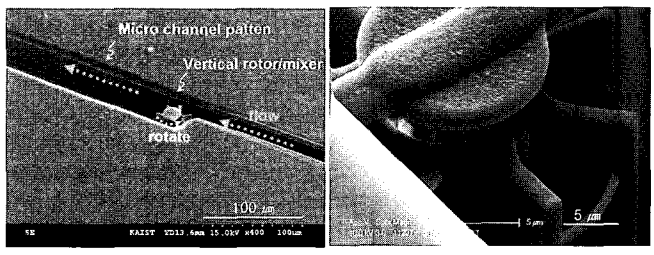

(a) (b)

Fig. 10 Fabricated micro-prototypes of a micro rotor

Figures 10(a) and (b) show SEM images of the fabricated structure. Active devices in microchannels could be fabricated simply using the proposed process. Novel 3D intelligent fluidic devices can be fabricated for μTAS (micro total analysis system) with high efficiency.

7. Summary

The two-photon stereolithography (TPS) process is a promising technique for the fabrication of 3D nano/micro structures. Recently, a number of research works have been conducted to overcome some obstacles to the application of the process to IT/BT industries. In this paper, we introduced our efforts in this area related to improvement of precision, fabrication speed, and functionality. In future works, neo-conceptive nano/micro devices using TPS, such as the 3D micro-channels suggested in this paper, will be developed and studied.

ACKNOWLEDGEMENT

The authors give thanks to Korean Ministry of Science & Technology (project of research for development of fundamental nanotechnology, M10503000217-05M0300-21700).

REFERENCES

1. Martin, Y., Rishton, S. and Wickramasinghe, H. K., "Optical Data Storage Read Out at 256 Gbits/in^2," Applied Physics Letters, Vol. 71, No. 1, pp. 1–3, 1997.

2. Toader, O. and John, S., "Proposed Square Spiral Microfabrication Architecture for Large Three-dimensional Photonic Band Gap Crystals," Science, Vol. 292, No. 1, pp. 1133–1135, 2001.

3. Stroock, A. D., Dertinger, S. K. W., Ajdari, A., Mezic, I., Stone, H. A. and Whitesides, G. M., "Chaotic mixer for microchannels," Science, Vol. 295, No. 25, pp. 647–651, 2002.

4. Henmi, N. and Tanaka, M., "An Open-Loop Method for Point-to-Point Positiong of a Piezoelectric Actuator," International Journal of Precision Engineering and Manufacturing, Vol. 8, No. 2, pp. 9–13, 2007.

5. Mizumoto, H., Yabuta, Y., Arii, S. and Tazoe, Y., "A Dual-Mode Pico-Positioning System Using Active Aerostatic Coupling," International Journal of Precision Engineering and Manufacturing, Vol. 8, No. 2, pp. 32–37, 2007.

6. Chou, S. Y., Krauss, P. R. and Renstrom, P. J., "Nanoimprint Lithography," J. Vac. Sci. Tech. B, Vol. 14, No. 6, pp. 4129–4133, 1996.

7. Jin, J. H., Misumi, I., Gonda, S. and Kurosawa, T., "Pitch Measurement of 150 nm 1D-grating Standards Using an Nano-Metrological Atomic Force Microscope," International Journal of Precision Engineering and Manufacturing, Vol. 5, No. 3, pp. 19–25, 2004.

8. Stilson, S., McClellan, A. and Devasia, S., "High-speed solution switching using piezo-based micropositioning stages," IEEE transactions on bio-medical engineering, Vol. 48, No. 7, pp. 806–814, 2001.

9. Adams, D. P., Mayer, T. M. and Swartzentruber, B. S., "Nanometer-scale Lithography on Si(001) using Adsorbed H as an Atomic Layer Resist," J. Vac. Sci. Tech. B, Vol. 14, No. 3, pp. 1642–1649, 1996.

10. Bjorholm, J. E., "EUV Lithography: The Successor to Optical Lithography," Intel Tech. Journal Q3, pp. 1–8, 1998.

11. Sung, I. H. and Kim, D. E., "Fabrication of Micro/nano-Patterns Using MC-SPL(Mechano-Chemical Scanning Probe Lithography) Process," International Journal of Precision Engineering and Manufacturing, Vol. 4, No. 5, pp. 22–26, 2003.

12. Lee, H. W., Han, C. S., Lee, E. S., Chul, Y., Kim, J. H., Kim, S. H. and Kwak, Y. K., "Direct Fabrication of the Scanning Probe Tip with Multi-Walled Carbon Nanotubes Using Dielectrophoresis," International Journal of Precision Engineering and Manufacturing,

Vol. 6, No. 2, pp. 50–54, 2005.

13. Campbell, M., Sharp, D. N., Harrison, M. T., Denning, R. G. and Turberfield, A. J., "Fabrication of Photonic Crystals for the Visible Spectrum by Holographic Lithography," Nature, Vol. 404, No. 6773, pp. 53–56, 2000.

14. Joannopoulos, J. D., "Self-assembly Lights up," Nature, Vol. 414, No. 6861, pp. 257–258, 2001.

15. Park, J. W., Ryu, S. H. and Chu, C. N., "Pulsed Electrochemical Deposition for 3D Micro Structuring," International Journal of Precision Engineering and Manufacturing, Vol. 6, No. 4, pp. 49–54, 2005.

16. Han, C. S., Seo, H. W., Lee, H. W., Kim, S. H. and Kwak, Y. K., "Electrokinetic Deposition of Individual Carbon Nanotube onto an Electrode Gap," International Journal of Precision Engineering and Manufacturing, Vol. 7, No. 1, pp. 42–46, 2006.

17. Shin, B. S., Kim, J. G., Chang, W. S. and Whang, K. H., "Rapid Manufacturing of 3D Micro-Products Using UV Laser Ablation and Phase-Change Filling," International Journal of Precision Engineering and Manufacturing, Vol. 7, No. 3, pp. 56–59, 2006.

18. Kawata, S., Sun, H. B., Tanaka, T. and Takada, K., "Finer features for functional microdevices," Nature, Vol. 412, No. 16, pp. 697–698, 2001.

19. Serbin, J., Egbert, A., Ostendorf, A., Chichkov, B. N., Houbertz, R., Domann, G., Schulz, J., Cronauer, C., Froehlich, L. and Popall, M., "Femtosecond laser-induced two-photon polymerization of inorganic-organic hybrid materials for applications in photonics," Optics Letters, Vol. 28, No. 5, pp. 301–303, 2003.

20. Maruo, S., Nakamura, O. and Kawata, S., "Three-dimensional microfabrication with two-photon-absorbed photopolymerization," Optics Letters, Vol. 22, No. 2, pp. 132–134, 1997.

21. Yang, D. Y., Park, S. H., Lim, T. W., Kong, H. J., Yi, Sh. W., Yang, H. K. and Lee, K. S., "Ultraprecise Microreproduction of a Three-Dimensional Artistic Sculpture by Multipath Scanning Method in Two-Photon Photopolymerization," Appl. Phys. Lett., Vol. 90, No. 1, pp. 013113, 2007.

22. Takada, K., Sun, H. B. and Kawata, S., "Improved spatial resolution and surface roughness in photopolymerization-based laser nanowriting," Appl. Phys. Lett., Vol. 86, No. 7, pp. 071122, 2005.

23. Seet, K. K., Mizeikis, V., Matsuo, S., Juodkazis, S. and Misawa, H., "Three-dimensional spiral-architecture photonic crystals obtained by direct laser writing," Advanced Materials, Vol. 17, No. 5, pp. 541–545, 2005.

24. Doraiswamy, A., Jin, C., Narayan, R. J., Mageswaran, P., Mente, P., Modi, R., Auyeung, R., Chrisey, D. B., Ovsianikov, A. and Chichkov, B., "Two Photon Polymerization of Organic-inorganic Hybrid Biomaterials for Microstructured Medical Devices," Acta Biomaterialia, Vol. 2, No. 3, pp. 267–275, 2006.

25. Lim, T. W., Park, S. H., Yang, D. Y., Kong, H. J. and Lee, K. S., "Direct Single-Layered Fabrication of 3D Concavo-Convex Patterns in Nano-Stereolithography," Applied Physics A, Vol. 84, No. 84, pp. 379–383, 2006.

26. Pham, T. A., Kim, D. P., Lim, T. W., Park, S. H., Yang, D. Y. and Lee, K. S., "Three-Dimensional SiCN Ceramic Microstructures via Nano-Stereolithography of Inorganic Polymer Photoresists," Advanced Functional Materials, Vol. 16, No. 9, pp. 1235–1241, 2006.

27. Park, S. H., Lim, T. W., Yang, D. Y., Jeong, J. H., Kim, K. D., Lee, K. S. and Kong, H. J., "Effective Fabrication of Three-Dimensional Nano/Microstructures in a single step Using Multilayered Stamp," Appl. Phys. Lett., Vol. 8, No. 20, pp. 203105, 2006.

28. Lim, T. W., Park, S. H., Yang, D. Y., Pham, T. A., Lee, D. H., Kim, D. P., Chang, S. I. and Yoon, J. B., "Fabrication of Three-Dimensional SiC-Based Ceramic Micropatterns Using a Sequential Micromolding-and-Pyrolysis Process," Microelectronic Engineeri-ng, Vol. 83, No. 11-12, pp. 2475–2481, 2006.

29. Park, S. H., Jeong, J. H., Choi, D. G., Kim, K. D., Altun, A. O., Lee, E. S., Yang, D. Y. and Lee, K. S., "Adaptive Bonding Technique for Precise Assembly of Three-Dimensional Microstructures," Applied Physics Letters, Vol. 90, No. 23, pp. 233109, 2007.

30. Teh, W. H., Durig, U., Salis, G., Harbers, R., Drechsler, U., Mahrt, R. F., Smith, C. G. and Guntherodt, H. J., "SU-8 for real three-dimensional subdifferaction-limit two-photon microfabrication," Appl. Phys. Lett., Vol. 84, No. 20, pp. 4095–4097, 2004.

31. Song, C. K., Shin, Y. J. and Lee, H. S., "Performance Assessment of an Ultraprecision Machine Tool Positioning System with a Friction Drive," International Journal of Precision Engineering and Manufacturing, Vol. 6, No. 3, pp. 8–12, 2005.

32. Saito, Y., Gao, W. and Kiyono, S., "A Single Lens Micro-Angle Sensor," International Journal of Precision Engineering and Manufacturing, Vol. 8, No. 2, pp. 14–19, 2007.

33. Fukada, S. and Nishimura, K., "Nanometric Positioning over a One-Millimeter Stroke Using a Flexure Guide and Electromagnetic Linear Motor," International Journal of Precision Engineering and Manufacturing, Vol. 8, No. 2, pp. 49–53, 2007.

34. Frolov, A. M., "Two-stage strategy for high-precision variational calculations," Physical review. A., Vol. 57, No. 4, pp. 2436–2439, 1998.

35. Park, J. W., Lee, D. W., Kawasegi, N. and Morita, N., "Nanoscale Fabrication in Aqueous Solution Using Tribo-Nanolithography," International Journal of Precision Engineering and Manufacturing, Vol. 7, No. 4, pp. 8–13, 2006.

36. Liao, C. Y., Bouriauand, M., Baldeck, P. L., Leon, J. C., Masclet, C. and Chung, T. T., "Two-dimensional Slicing Method to Speed up the Fabrication of Micro Objects Based on Two-photon Polymerization," Appl. Phys. Lett., Vol. 91, No. 3, pp. 033108, 2007.

37. Yoo, D. J., "Filling Holes in Large Polygon Models Using an Implicit Surface Scheme and the Domain Decomposition Method," International Journal of Precision Engineering and Manufacturing, Vol. 8, No. 1, pp. 3–10, 2007.

38. Yang, H., Deschatelets, P., Brittain, S. T. and Whitesides, G. M., "Fabrication of high performance ceramic microstructures from a polymeric precursor using soft lithography," Advanced Materials., Vol. 13, No. 1, pp. 54–58, 2001.

39. Liew, L. A., Liu, Y., Luo, R., Cross, T., An, L., Bright, V. M., Dunn, M. L., Daily, J. W. and Raj, R., "Fabrication of SiCN MEMS by photopolymerization of pre-ceramic polymer," Sensors and Actuators A, Vol. 95, No. 2, pp. 120–134, 2002.

40. Provin, C., Monneret, S., Gall, H. L. and Corbel, S., "Three-dimensional ceramic microcomponents made using microstereo-lithography," Advanced Materials, Vol. 15, No. 12, pp. 994–997, 2003.